

# Two-Photon Fluorescence Microscopy of Corneal Riboflavin Absorption

Daniel M. Gore,<sup>1</sup> Anca Margineanu,<sup>2</sup> Paul French,<sup>2</sup> David O'Brart,<sup>3</sup> Chris Dunsby,<sup>2</sup> and Bruce D. Allan<sup>1</sup>

<sup>1</sup>Moorfields Eye Hospital, London, United Kingdom

<sup>2</sup>Department of Physics, Imperial College, South Kensington, London, United Kingdom

<sup>3</sup>Department of Ophthalmology, St. Thomas' Hospital, London, United Kingdom

Correspondence: Daniel M. Gore, External Disease Service, Moorfields Eye Hospital, 162 City Road, London EC1V 2PD, UK; dan.gore@moorfields.nhs.uk.

Submitted: January 18, 2014

Accepted: March 10, 2014

Citation: Gore DM, Margineanu A, French P, O'Brart D, Dunsby C, Allan BD. Two-photon fluorescence microscopy of corneal riboflavin absorption. *Invest Ophthalmol Vis Sci*. 2014;55:2476-2481. DOI:10.1167/iov.14-13975

**PURPOSE.** To correct for attenuation in two-photon fluorescence (TPF) measurements of riboflavin absorption in porcine corneas.

**METHODS.** Two-photon fluorescence imaging of riboflavin was performed using excitation at a wavelength of 890 nm, with fluorescence signal detected between 525 and 650 nm. TPF signal attenuation was demonstrated by imaging from either side of a uniformly soaked corneoscleral button. To overcome this attenuation, a reservoir of dextran-free 0.1% wt/vol riboflavin 5'-monophosphate in saline and hydroxypropyl methylcellulose (HPMC) was placed on top of porcine corneas (globe intact-epithelium removed). TPF imaging was performed through this reservoir with image stacks acquired at 10- $\mu$ m steps through the cornea repeated at regular intervals for up to 60 minutes. A novel correction method was applied to achieve corneal riboflavin concentration measurements in whole eyes ( $n = 4$ ).

**RESULTS.** Significant attenuation of the TPF signal was observed in all eyes, with the signal decreasing approximately linearly with depth in uniformly soaked tissue. Cross-sectional TPF images taken of excised corneal strips confirmed the tissue was uniformly soaked so that the decrease in signal was not due to spatial variations in riboflavin concentration. After correcting for signal attenuation, we observed increased riboflavin concentrations with longer soak duration, with the mean (standard deviation) maximum tissue concentration recorded at 0.094% ( $\pm 0.001$ ) wt/vol [1.36 mg/mL]. Uniform riboflavin absorption was achieved after a minimum 50 minutes. Following a standard corneal cross-linking soak of 30 minutes, a mean stromal concentration of 0.086% ( $\pm 0.001$ ) wt/vol [1.25 mg/mL] was achieved at a depth of 300  $\mu$ m.

**CONCLUSIONS.** The accuracy of TPF measurements of corneal riboflavin absorption can be increased by applying a correction for depth-related signal attenuation.

**Keywords:** cross-linking, riboflavin, two-photon fluorescence microscopy, concentration, corneal stroma

Keratoconus is a condition in which the corneal shape becomes steeper and more irregular between childhood and the mid-thirties. It is a common cause of visual impairment in young people, with a prevalence estimated at 1 in 1750 in white Europeans and 1 in 440 in Asians.<sup>1</sup> As the corneal shape becomes more abnormal, first spectacles, then rigid contact lenses become ineffective. Prior to the availability of newer surgical interventions, including corneal collagen cross-linking (CXL) and intrastromal corneal ring segments, up to 20% of patients eventually required a corneal transplant to correct vision.<sup>2</sup>

CXL is the first treatment available to halt disease progression in keratoconus. It is effective in over 90% of treated eyes, and may also result in improvements in corneal shape and vision.<sup>3-8</sup> CXL is performed by irradiating riboflavin-soaked corneal tissue with an ultraviolet A (UVA) light source (370 nm). The riboflavin acts both as a photosensitizer to encourage UVA-induced corneal stiffening (cross-linking), and a shield to reduce UVA levels at the endothelial level below the cytotoxic threshold. The original CXL protocol<sup>9</sup> described

removal of the corneal epithelium with application of riboflavin 0.1% drops 5 minutes before, and every 5 minutes during, UVA treatment (3 mW/cm<sup>2</sup> power for 30 minutes).

The optimum riboflavin soak duration and concentration in the cornea required to achieve effective collagen cross-linking is unknown. Originally, slit-lamp biomicroscopy was used in patients to check for riboflavin fluorescence in the aqueous as a surrogate marker of complete corneal stromal penetration. Confocal and two-photon fluorescence (TPF) microscopy have both been used to quantify the concentration and 3-dimensional distribution of riboflavin in feline,<sup>10</sup> chick embryo,<sup>11</sup> and porcine<sup>12,13</sup> corneas. Advantages for TPF include reduced bleaching and phototoxicity outside the focal point, making it easier to obtain quantitative, 3D measurements, and reduced attenuation of the excitation light in the target medium due to its longer wavelength.

Near-absence of TPF signal attenuation has been demonstrated within a microfluidic system.<sup>14</sup> In tissue, however, a number of additional factors, principally scattering and aberration, may cause TPF signal loss with increasing scan

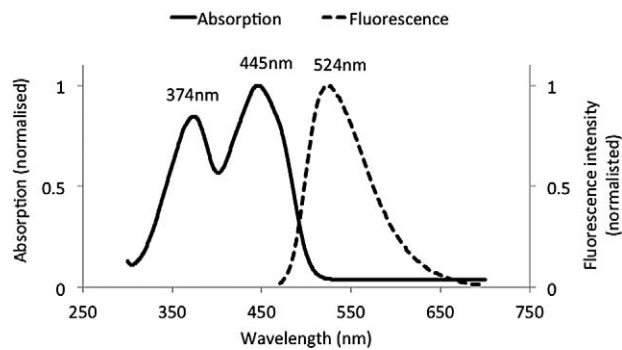


**FIGURE 1.** The absorption and fluorescence emission spectra of dextran-free 0.1% riboflavin 5'-monophosphate in saline and HPMC (Avedro, Inc.). Absorption peaks are seen at 374 nm and 445 nm; a fluorescence emission peak is seen at 524 nm when excited at 445 nm.

depth.<sup>10,12</sup> While acknowledging this problem, Cui et al.<sup>10</sup> made no correction for signal attenuation with increasing scan depth in their application of TPF imaging to the measurement of riboflavin concentration in (feline) corneas.

In this paper, we aimed to explore TPF signal attenuation in uniformly saturated corneas, and to derive a correction for this attenuation designed to enhance the accuracy of experimental measurements of riboflavin concentration at different depths within the cornea using variations in soak protocol.

## MATERIALS AND METHODS

### Riboflavin Spectrophotometry

The fluorescence absorption and emission spectra of 0.1% wt/vol riboflavin 5'-monophosphate (1.45 mg/mL) in saline and hydroxypropyl methylcellulose (HPMC; VibeX Rapid; Avedro, Inc., Waltham, MA, USA) were measured by spectrophotometry (UV-3101PV UV-VIS-NIR; Shimadzu, Kyoto, Japan). Riboflavin exhibited a bimodal absorption spectrum with a lower peak at 374 nm, and a higher peak at 445 nm (Fig. 1). The maximum emission wavelength was 524 nm.

### Two-Photon Microscope Setup

A Ti:Sapphire laser (Chameleon Vision II; Coherent, Inc., Santa Clara, CA, USA) equipped with a prism-based group velocity dispersion (GVD) compensation unit was used as the excitation laser source. The laser has a tuning range from ~680 nm up to 1080 nm, operating with a 140-fs pulse duration and 80-MHz pulse repetition rate. The excitation laser beam was guided to a upright microscope (Leica DM6000CS; Leica Microsystems GmbH, Wetzlar, Germany) via an electro-optical modulator (EOM) to control laser output and coupled into the spectral scan-head (Leica SP8; Leica Microsystems GmbH) where it passes through two galvanoscanners, allowing scanning in the *x-y* plane, before being focused into the sample by a Leica  $\times 25/0.95$  NA water immersion objective (coverslip corrected) that facilitated a working depth of up to 2 mm. Theoretical (full-width half-maximum) resolutions were calculated at 0.34  $\mu\text{m}$  laterally and 1.4  $\mu\text{m}$  axially. We used two-photon excitation at 890 nm and the emitted fluorescence passed through an 800-nm short pass dichroic filter (Chroma Technology Corp., Bellows Falls, VT, USA), which was then spectrally separated by a beam splitter (Leica Acousto-Optic-Beam Splitter [AOBS]; Leica Microsystem GmbH) before passing through the Leica HyD detectors.

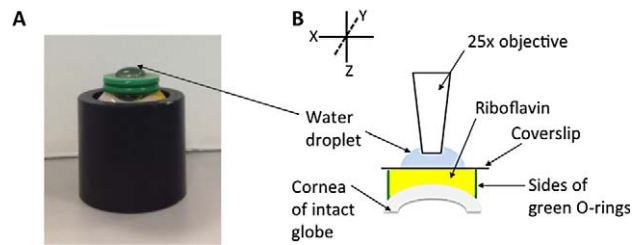


**FIGURE 2.** Intact globe set-up on microscope stage. (A) Perspex cylinder used to secure whole globe on the microscope stage with a sealed, air bubble free reservoir of riboflavin on top of the cornea (B).

### Sample Preparation

Freshly enucleated porcine eyes (First Link, Ltd., Wolverhampton, UK), stored within a sealed bottle of phosphate buffered saline (0.85% NaCl, 0.01M NaPhos, pH 7.2-7.4), were transported on ice to arrive within 24 hours of death. Each globe was secured within a custom-made Poly(methyl methacrylate) cylinder (Perspex; Perspex Distribution, Ltd., Blackburn, UK) to ensure stability on the microscope stage (Fig. 2A). A custom reservoir chamber for riboflavin (a coverslip glued onto two rubber O-rings) was placed coverslip down and filled with ~400  $\mu\text{L}$  of riboflavin solution. After epithelial removal using a hockey stick scraper (e.janach srl, Como, Italy), the cornea of the intact globe was apposed to the O-ring and immersed in riboflavin and a timer was started (time = 0 minutes). The assembly was then inverted, creating a bubble-free, sealed lake of riboflavin over the cornea and beneath the coverslip ready for imaging (Fig. 2B). The assembly was then positioned within a custom-built recessed stage to house the cylinder-supported globes beneath the objective. The first TPF z-stack was started at time = 2.5 minutes.

### Imaging Protocol and Concentration Calibration

TPF excitation light of 890-nm wavelength was chosen to correspond with the highest riboflavin absorption peak (445 nm) as determined by spectrophotometry. The average laser output power at 890 nm was 33 mW at the objective with minimal fluctuation in average power being observed during the course of any given day's experiment. Emitted riboflavin fluorescence was collected between 525 nm and 650 nm, to avoid overlap with the absorption spectrum of riboflavin. We confirmed the absence of any reabsorption of this emitted light by demonstrating no change in measured TPF signals with excitation depth in homogeneous riboflavin solutions within a well slide (Fig. 3).

Serial z-stacks at 10- $\mu\text{m}$  intervals were started within the precorneal riboflavin reservoir at approximately 30  $\mu\text{m}$  above the corneal surface to provide a reference TPF signal level for this 0.1% wt/vol solution. This level provided a signal-to-concentration calibration for each eye. Z-stacks were acquired through the depth of the cornea (scan rate: 600 Hz, 512  $\times$  512 pixels, image size: 445  $\mu\text{m}$   $\times$  445  $\mu\text{m}$ , line average: 2, pinhole wide open, ~130 seconds total acquisition). Each run was repeated every 2.5 minutes, up to 20 minutes, and then every 5 minutes, up to 60 minutes.

### Confirming TPF Signal Attenuation

To demonstrate that TPF signal attenuation must be occurring when imaging en face, we excised corneal strips from riboflavin-soaked intact globes. A cross-sectional surface of each strip was placed face-down onto a microscope slide and a coverslip was placed on top. A single TPF image (using a 10  $\times$

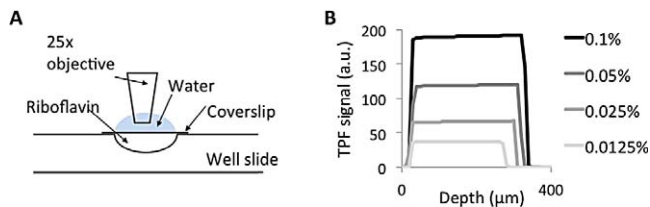


**FIGURE 3.** TPF signal calibration for riboflavin in solution. (A) Well slide setup beneath a coverslip-corrected objective. (B) Serial riboflavin dilutions from 0.1% to 0.0125% (wt/vol) produced constant TPF signals with depth through the drop sample.

0.30 NA objective) was acquired of a plane approximately 50  $\mu\text{m}$  below the coverslip. Excised corneoscleral buttons were also imaged from both directions, draped over a scleral contact lens to avoid stromal folds. A coverslip was then placed directly on top, applanating a central area of the cornea without coupling fluid, and  $z$ -stacks of TPF images were acquired. No immersion fluid was used for either excised tissue experiment to minimize the migration of riboflavin within the cornea prior to imaging. The time taken to excise and mount the tissue prior to imaging was under 2 minutes. Results from both these experiments were compared with  $z$ -stacks acquired in intact globes.

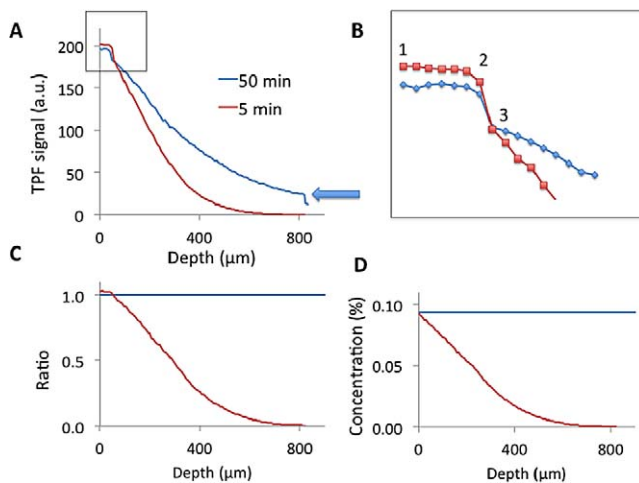


**FIGURE 4.** Example methodology of correcting TPF signal attenuation when imaging intact globes. (A) Spatially ( $x$ - $y$ ) averaged raw TPF data for 5- and 50-minute soak durations in the same eye plotted against corneal depth ( $z$ ). After 50 minutes the TPF signal recorded at the back of the cornea (blue arrow) plateaued, with no further increases observed at 55 or 60 minutes (plots not shown). This indicated the tissue was completely and uniformly soaked, with attenuation of the signal preventing a flat signal plot. This 50-minute plot was used to model the signal attenuation. (B) Enlarged box insert from (A) delineating the changes in signal slope at the beginning of the  $z$ -stack: 1 to 2 is within the precorneal riboflavin reservoir; 2 to 3 is part-cornea, part-reservoir; 3 onwards, the whole of the image is within the cornea. (C) All TPF signal readings at 5 minutes were then divided by the reading for the corresponding depth in the 50-minute plot (uniformly saturated), giving a uniform corrected TPF signal level throughout the cornea for the 50-minute plot and a corrected slope for the earlier time point. (D) The  $y$ -axis of the plot was converted to riboflavin concentration by normalizing to the TPF signal level within the reservoir of 0.1% riboflavin solution. The  $x$ -axis of the plot was shifted so that a depth of 0  $\mu\text{m}$  corresponded with the start of the cornea.

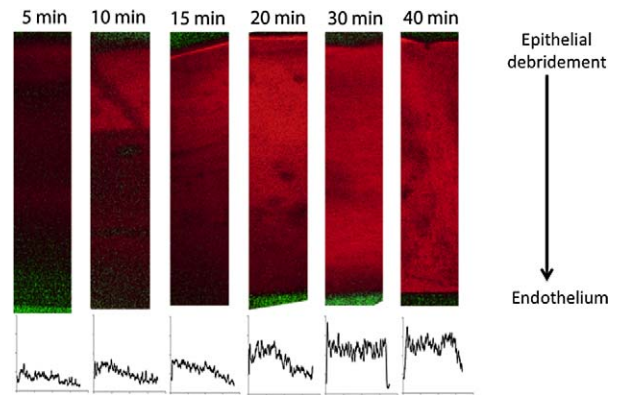


**FIGURE 5.** TPF images of cross-section of excised corneal strips showing increasingly uniform TPF signal with longer soak times. Plots of TPF signal variation across the sectioned corneal specimens, produced using Java-based imaging software (ImageJ, 1.47v, <http://imagej.nih.gov/ij>; provided in the public domain by the National Institutes of Health, Bethesda, MD, USA); are shown below each strip. These images confirm that the signal drop observed with increasing depth in uniformly soaked corneal specimens on  $z$ -stack imaging was attributable to signal attenuation rather than any variation in riboflavin concentration with depth. Excising strips of cornea was inevitably complicated by aqueous loss which is likely to wash and dilute some of the riboflavin from the tissue. In addition significant distortion of the tissue was observed when laid face-up on a slide (the images presented have been rescaled to the thicknesses observed on  $z$ -stack imaging prior to excision). This method is not suitable for quantifying TPF signals.

### TPF Signal Correction

The average raw TPF signal data for each image in a  $z$ -stack were exported in .CSV format (Excel for Mac, 2011; Microsoft Corp, Redmond, WA, USA) and plotted against corneal depth for measurements with corneas soaked for increasing times. A uniform concentration of riboflavin was judged to have been achieved when the posterior corneal TPF signal stopped increasing (typically after  $\sim 50$  minutes). The  $z$ -stack data for this condition was then used to provide the attenuation reference for this eye (i.e., each eye provided its own internal reference). A detailed example using this methodology to correct the attenuation at earlier time points is shown in Figure 4.

## RESULTS

### Proof of TPF Signal Attenuation

Cross-sectional TPF images (Fig. 5) taken of excised corneal strips demonstrated near-uniform signals after a 40-minute soak. After a 60-minute soak to ensure uniform saturation, the TPF signal was seen to diminish with depth in the cornea in an excised corneoscleral button (Fig. 6). Although the relative amplitude of the TPF signal was reduced compared with the intact globe image prior to excision, reversing the tissue (i.e., endothelial side up) did not reverse the slope of the TPF signal loss, confirming that the decrease in TPF signal when imaging through the  $z$ -axis is due to signal attenuation rather than a depth-dependent drop in riboflavin concentration.

### Time and Dose-Dependent Corrected Corneal Riboflavin Concentrations

After correcting for this signal attenuation, we observed that TPF signals increased with longer riboflavin soak duration,



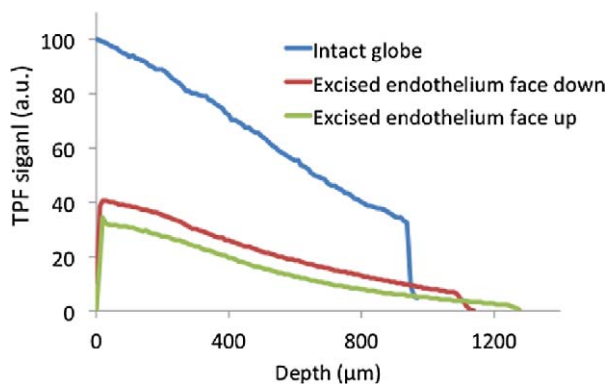


**FIGURE 6.** Corneal TPF imaging through a uniformly soaked globe (control, 60 minutes). A corneoscleral button was then excised and draped over a scleral contact lens to maintain relative corneal curvature (with a coverslip on top) before repeating the TPF z-stack. The button was then re-laid endothelium facing up. Note that the slope does not reverse when the same corneal specimen is reimaged endothelium face-up. This is further evidence that the drop in TPF signal level with increasing tissue depth on z-stack images of a uniformly soaked specimen is attributable to signal attenuation rather than any variation in riboflavin concentration. We postulate that the large drop in TPF signal observed for excised tissue, and the further small drop when the same specimen is reverse mounted, are attributable to increased light scatter when the corneal tissue architecture is distorted, despite trying to minimize this with a contact lens support. The same distortion also caused bunching of the tissue such that the thickness appeared to increase as compared to imaging the globe intact.

with the mean ( $\pm$ SD) maximum tissue concentration recorded at 0.094% ( $\pm$ 0.0008) wt/vol (1.36 mg/mL; Figs. 7, 8). Uniform riboflavin absorption across the entire corneal depth was achieved after a minimum 50 minutes (range, 50–55 minutes). Following a 30-minute soak, as commonly used in epithelium-off CXL protocols, a mean stromal concentration of 0.086% ( $\pm$ 0.001) wt/vol (1.25 mg/mL) was achieved at a depth of 300  $\mu$ m. Half this concentration (0.043% [ $\pm$  0.014] wt/vol, 0.62 mg/mL) was observed within the first 5 minutes. Without correcting for attenuation, the concentration after 30 minutes at 300  $\mu$ m was calculated at 0.06%.

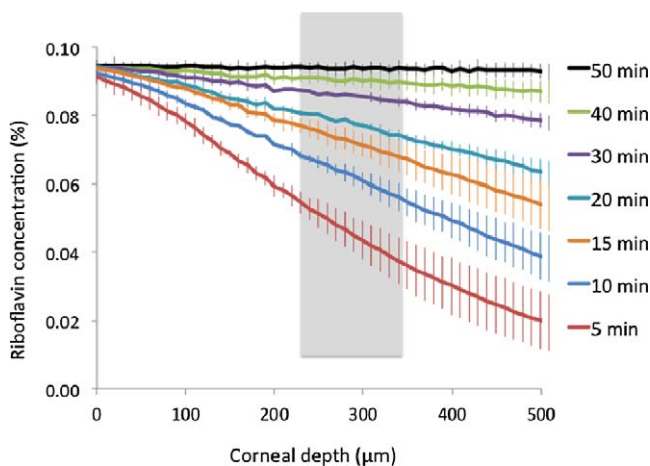


**FIGURE 7.** Mean riboflavin concentrations, corrected for TPF signal attenuation, presented over a 500- $\mu$ m depth corresponding to the approximate thickness of a human cornea after epithelial removal ( $n = 4$ , standard deviation error bars). The shaded box highlights the demarcation zone between 250 and 350  $\mu$ m commonly seen after epithelium-off corneal cross-linking in human corneas.

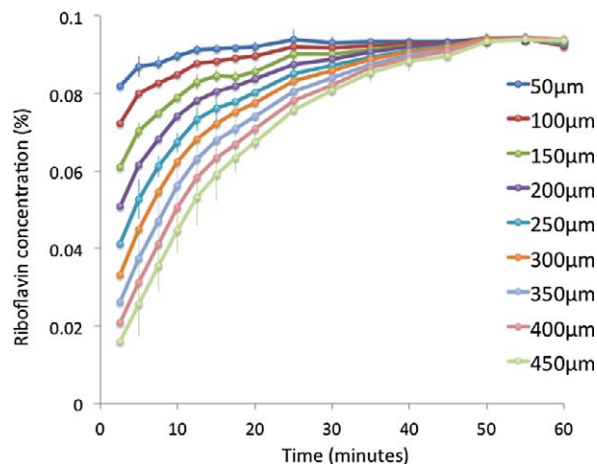


**FIGURE 8.** Mean changes in corneal riboflavin concentration, corrected for TPF signal attenuation, at different depths ( $n = 4$ , alternate plot standard deviation error bars).

**DISCUSSION**

We have shown that the riboflavin TPF signal is attenuated with increasing depth in corneal tissue and demonstrated a correction method designed to increase measurement accuracy for ex vivo comparisons of riboflavin absorption for different soak protocols.

There are a number of potential causes of increased TPF signal attenuation with depth, including absorption and scattering of both excitation and emission radiation and aberration of the excitation beam focus. Fluorescence photons emitted at wavelengths corresponding to the overlap between the absorption and emission spectra (Fig. 1) can be reabsorbed. This “inner-filter” effect is more pronounced the higher the concentration of fluorescence photons in the sample. As such, when fluorescence microscopy is used to determine fluorophore concentration, fluorescence intensity will only be proportional to the concentration at less-concentrated solutions. We initially observed this effect at the highest (0.1%) riboflavin concentration, with an increasingly attenuated signal when imaging through calibration drops on a well slide. By shifting the microscope detector range beyond the riboflavin absorption spectrum ( $>525$  nm), we minimized this phenomenon, obtaining near-flat TPF signals with increasing depth through the drop (Fig. 3B).

Previous studies using TPF microscopy to quantify corneal riboflavin absorption ignore the inner-filter effect. Cui et al.<sup>10</sup> measured both fluorescein and riboflavin absorption in feline corneas, and while the effects of reabsorption of the fluorescence emitted from fluorescein were mitigated by a bandpass filter of appropriate wavelength, no such detection filter was used for the riboflavin measurements. By way of a signal attenuation correction factor, Kampik et al.<sup>12</sup> used the intensity loss in collagen fiber second-harmonic generation (SHG) signals taken simultaneously during the same z-scan. However, the SHG detector wavelength channel used (420–460 nm), and to a lesser extent that used for riboflavin (505–555 nm), overlap with the absorption spectrum of riboflavin (300–525 nm; Fig. 1). This would be expected to cause significant reabsorption of the emitting SHG light, compromising its use a reference to correct TPF signal attenuation.

Our calibration method is based on two assumptions: first, that the concentration within the riboflavin reservoir above the cornea remains constant throughout the entire soak; and second, that in a fully soaked cornea, the riboflavin concentration within the cornea equals that of the reservoir. In

practice, however, these assumptions may not be strictly correct. Figure 4B reveals that the TPF signal within the reservoir does decrease with time, albeit by only a few percent. With a finite (small) volume, the reservoir is potentially susceptible to photobleaching. We investigated this by repeating the above z-stack protocol through the same custom chamber reservoir of riboflavin placed on a slide (i.e., no cornea). Over 50 minutes we observed near-identical TPF signal plots over a depth of 1200  $\mu\text{m}$ , with no evidence of photobleaching. We have additionally investigated the possibility of photobleaching within the corneal tissue, by performing a final z-stack at the end of the full 60 minute protocol in a new adjacent axial location (i.e., unirradiated tissue). We observed near identical TPF signal plots over a depth of 800  $\mu\text{m}$ , with no evidence of photobleaching. Fluorescence excitation restricted to the focal plane is a key advantage of multi-photon microscopy, explaining the lack of photobleaching demonstrated. An alternative explanation could be that the reduction in TPF signal with time is due to loss of fluorescent riboflavin molecules as they diffuse into the cornea. However, as illustrated Figure 4B, this decrease over 50 minutes was small, with a mean of 2.5% ( $\pm 1.1$ ) for all imaged eyes. For future work, this small effect could be reduced by increasing the volume of the reservoir. The assumption that the concentration in a fully soaked cornea is the same as that in the reservoir also appears to be not quite correct. We consistently observed a step-like decrease in TPF signal as the imaged plane transitioned from the fluid-filled reservoir into the cornea (Fig. 4B), measured to be 6.1% ( $\pm 1.6$ ) after a 50-minute soak. This small loss of signal may result from optical aberrations encountered as the laser light crosses the curved surface of the cornea or it may reflect a true difference in concentration between the reservoir and the fully soaked cornea.

The percentage transmission of light of wavelengths between 600 nm and 1000 nm has been previously measured in early postmortem eyes between 95% and 98%.<sup>15</sup> Scattering of light may still occur in an otherwise healthy optical system, becoming more prevalent in disease (for example cataract, corneal edema or corneal scarring). Edema is likely to be particularly relevant in the porcine corneas used in this current study which, although optically clear to the naked eye, were regularly over 800  $\mu\text{m}$  in central corneal thickness (pre-riboflavin soak), compared with published in vivo measurements of  $666 \pm 68 \mu\text{m}$ .<sup>16</sup> This is presumed to be due to early endothelial failure within the first 24 hours after harvest and is a limitation of this animal model.

There is a lack of consensus regarding the exact nature and location of CXL-induced collagen cross-links.<sup>17,18</sup> Two-photon microscopy of corneal collagen has been used in an in vivo rabbit model to quantify corneal collagen cross-links after treatment.<sup>19</sup> In this study, the investigators identified a well-demarcated change in both autofluorescence and SHG signal down to a depth of 250  $\mu\text{m}$ . This correlates well with a demarcation line visible by optical coherence tomography (OCT) in human patients, typically around 250 to 300  $\mu\text{m}$  after epithelium-off CXL.<sup>20,21</sup> At this depth (300  $\mu\text{m}$ ), following a standard 30-minute soak, we measured a mean stromal concentration of 0.086%. It is, however, not possible to make any absolute correlation between the concentrations reported in our study (using an HPMC-based riboflavin preparation) and demarcation line tissue changes observed in vivo on OCT (using a dextran-based riboflavin preparation). We attempted to apply our methodology to determine concentration depth profiles using 0.1% riboflavin in 20% dextran (500 kDa) as used in the original CXL study,<sup>9</sup> in both well-slide and soaked corneas, but were unable to achieve any consistent TPF signals. Dextran has previously been shown to strongly absorb near-infrared light<sup>22</sup> and absorption of the TPF excitation beam may

have been raising the temperature of dextran and affecting its optical properties. This is likely to have been the cause of variations in the TPF signal levels we measured. TPF microscopy may therefore not be suitable to investigate corneal riboflavin absorption for dextran-based preparations. We note that these are being replaced by HPMC-based preparations which appear to have faster tissue diffusion rates<sup>23</sup> as well as causing less corneal thinning during treatment.<sup>24</sup>

In conclusion, we present evidence that TPF microscopy of corneas in an ex vivo animal model is affected by significant signal attenuation when imaging at depth. To account for this, we have presented a new time-lapse measurement approach carried out during the riboflavin soak in which each cornea acts as its own internal reference. Correction for TPF signal attenuation should enhance the accuracy of experimental riboflavin absorption measurements used to guide the development of clinical protocols for CXL.

### Acknowledgments

The authors thank Christopher Thrasivoulou, imaging team manager at the University College London confocal unit, for microscopy technical support; Thomas van den Berg (Netherlands Institute for Neuroscience) for personal correspondence regarding corneal light transmittance; and Grace Lyttle, Avedro, Inc., for provision of riboflavin solution and methodological support.

Supported by Fight for Sight (1348/9 [DMG, PF, CD, BDA]); the Rosetrees Trust (JS16/M282 [DMG]); and the Ian Collins Rayner Fellowship (Rayner Intraocular lenses Ltd., United Kingdom and Ireland Society of Cataract and Refractive Surgeons [DMG]).

Disclosure: **D.M. Gore**, Avedro, Inc. (F); **A. Margineanu**, None; **P. French**, None; **D. O'Brart**, None; **C. Dunsby**, None; **B.D. Allan**, None

### References

- Pearson A, Soneji B, Sarvanathan N. Does ethnic origin influence the incidence or severity of keratoconus? *Eye*. 2000; 14:625-628.
- Lass JH, Lembach RG, Park SB, et al. Clinical management of keratoconus. A multicenter analysis. *Ophthalmology*. 1990;97: 433-445.
- Caporossi A, Mazzotta C, Baiocchi S, Caporossi T. Long-term results of riboflavin ultraviolet a corneal collagen cross-linking for keratoconus in Italy: the Siena eye cross study. *Am J Ophthalmol*. 2010;149:585-593.
- Wittig-Silva C, Whiting M, Lamoureux E, Lindsay RG, Sullivan LJ, Snibson GR. A randomized controlled trial of corneal collagen cross-linking in progressive keratoconus: preliminary results. *J Refract Surg*. 2008;24:S720-S725.
- O'Brart DPS, Chan E, Samaras K, Patel P, Shah SP. A randomised, prospective study to investigate the efficacy of riboflavin/ultraviolet A (370 nm) corneal collagen cross-linkage to halt the progression of keratoconus. *Br J Ophthalmol*. 2011;95:1519-1524.
- Hersh PS, Greenstein SA, Fry KL. Corneal collagen crosslinking for keratoconus and corneal ectasia: one-year results. *J Cataract Refract Surg*. 2011;37:149-160.
- Koller T, Mrochen M, Seiler T. Complication and failure rates after corneal crosslinking. *J Cataract Refract Surg*. 2009;35: 1358-1362.
- Gore DM, Shortt AJ, Allan BD. New clinical pathways for keratoconus. *Eye (Lond)*. 2013;27:329-339.
- Wollensak G, Spoerl E, Seiler T. Riboflavin/ultraviolet-a-induced collagen crosslinking for the treatment of keratoconus. *Am J Ophthalmol*. 2003;135:620-627.

10. Cui L, Huxlin KR, Xu L, MacRae S, Knox WH. High-resolution, noninvasive, two-photon fluorescence measurement of molecular concentrations in corneal tissue. *Invest Ophthalmol Vis Sci.* 2011;52:2556-2564.
11. Zhang Y, Sukthankar P, Tomich JM, Conrad GW. Effect of the synthetic NC-1059 peptide on diffusion of riboflavin across an intact corneal epithelium. *Invest Ophthalmol Vis Sci.* 2012;53:2620-2629.
12. Kampik D, Ralla B, Keller S, Hirschberg M, Friedl P, Geerling G. Influence of corneal collagen crosslinking with riboflavin and ultraviolet-a irradiation on excimer laser surgery. *Invest Ophthalmol Vis Sci.* 2010;51:3929-3934.
13. Søndergaard AP, Hjortdal J, Breitenbach T, Ivarsen A. Corneal distribution of riboflavin prior to collagen cross-linking. *Curr Eye Res.* 2010;35:116-121.
14. Schafer D, Gibson EA, Amir W, et al. Three-dimensional chemical concentration maps in a microfluidic device using two-photon absorption fluorescence imaging. *Opt Lett.* 2007;32:2568-2570.
15. Beems EM, Van Best JA. Light transmission of the cornea in whole human eyes. *Exp Eye Res.* 1990;50:393-395.
16. Hatami-Marbini H, Etebu E, Rahimi A. Swelling pressure and hydration behavior of porcine corneal stroma. *Curr Eye Res.* 2013;38:1124-1132.
17. Hayes S, Kamma-Lorger CS, Boote C, et al. The effect of riboflavin/UVA collagen cross-linking therapy on the structure and hydrodynamic behaviour of the ungulate and rabbit corneal stroma. *PLoS One.* 2013;8:e52860.
18. Wollensak G, Wilsch M, Spoerl E, Seiler T. Collagen fiber diameter in the rabbit cornea after collagen crosslinking by riboflavin/UVA. *Cornea.* 2004;23:503-507.
19. Krüger A, Hovakimyan M, Ramirez Ojeda DF, et al. Combined nonlinear and femtosecond confocal laser-scanning microscopy of rabbit corneas after photochemical cross-linking. *Invest Ophthalmol Vis Sci.* 2011;52:4247-4255.
20. Seiler T, Hafezi F. Corneal cross-linking-induced stromal demarcation line. *Cornea.* 2006;25:1057-1059.
21. Doors M, Tahzib NG, Eggink FA, Berendschot TTJM, Webers CAB, Nuijts RMMA. Use of anterior segment optical coherence tomography to study corneal changes after collagen cross-linking. *Am J Ophthalmol.* 2009;148:844-851.
22. Xu X, Wang RK, Elder JB, Tuchin VV. Effect of dextran-induced changes in refractive index and aggregation on optical properties of whole blood. *Phys Med Biol.* 2003;48:1205-1221.
23. Marshall J, Hersh P, Muller D. 2013. Corneal Collagen Cross-Linking: Past, Present, Future. 2013:71-73. Available at: <https://www.dropbox.com/sh/yw1zcicu0mwwmur/U5Vn3Ulb9e>. Accessed February 21, 2014.
24. Cinar Y, Cingü AK, Sahin A, Türkcü FM, Yüksel H, Caca I. Intraoperative corneal thickness measurements during corneal collagen cross-linking with isotonic riboflavin solution without dextran in corneal ectasia. *Cutan Ocul Toxicol.* 2014;33:28-31.